12. **Taranov, V.G.**(2005) *Some problems of the founding of the powerful turbo-generator sets* / V. G. Taranov, N. S. Shvetz, V. B. Shvetz // Pros. 16 ICSMGE.- 2005.- Osaka. - vol. 3. – P. 1567- 1570.
13. SNiP 2.02.05–87 Foundations of machines with dynamic loads:− Adopted:01/01/1985. - 32 c.
14. DSTU B B.2.1-17: 2009. Foundations and foundations of buildings and structures. Soils. Methods of laboratory determination of physical properties. Adopted: 02/08/2018 Date: 01/01/2019 - 36 p.

# PHYSICAL-CHEMICAL AND TECHNOLOGICAL PARAMETERS OF IMPROVING PROFITABILITY OF UNDERGROUND COAL BURNING

**Inkin O. V.**
Doctor of Technical Sciences, Professor at Department of the Hydrogeology and Engineering Geology, Dnipro University of Technology, Dnipro, Ukraine

**Puhach A. M.**
Doctor of Public Administration, Dnipro State Agrarian and Economic University, Dnipro, Ukraine

**Dereviahina N. I.**
Candidate of Technical Sciences, Associate Professor at Department of Hydrogeology and Engineering Geology, Dnipro University of Technology, Dnipro, Ukraine

**Abstract.** Currently, coal is the main natural energy carrier in Ukraine due to its limited resources of oil and natural gas. A promising method for extracting coal is underground gasification using thermochemical and mass-exchange processes. Objective of the paper is to substantiate and implement the integrated approach aimed at the studies of filtration and mass-transfer processes within roof rocks of coal seams in the context of their underground gasification. Integrity of the studies is substantiated by the use of analytical calculations as well as physical and numerical modeling. Zones with different permeability have been determined and values of specific water inflow have been identified basing upon the performed numerical modeling and involving multicomponent transformations within roof formation.The research data actuality is in the studies of spatial and temporal dynamics of rock technogenic rock permeability above gasification channel depending upon their geological structure which will favour the substantiation of efficient engineering solutions to control a process of underground coal gasification under difficult hydrogeological conditions. It has been substantiated that almost all disturbing factors have negative effect on gas calorifity whereas parameters of blast rate increase and static pressure growth in a gas generator have the most positive effect among the controlling factors. Aspects concerning the increase in loss of the produced gas that may reduce economic efficiency and environmental safety of underground coal gasification have been considered as well. Using the results, we improved the UCG technology by using the condensing products of gasification in the overburden.

**Introduction**. The necessity to make a technique of coal extraction, conversion, and use more ecologically feasible on the crucially new basis, while minimizing the environmental impact and reducing waste volume, is one of the topical problems to be solved by energy sector of Ukraine. Underground coal gasification (UCG) is the innovative solution to the problem. The process relies upon the transition of a mineral into a movable gas-condensate state within its occurrence by means of thermochemical and mass-exchange reactions. Gasification is followed by the loss of gas, being formed, into enclosing rocks which value is influenced by a number of factors. In this context, gas loss may achieve 30% affecting ecological compatibility and efficiency of UCG significantly. Thus, object of the paper is to study the parameters affecting the process of underground coal gasification as well as gas loss into roof rocks of underground gas generator.

**Statement of basic material of the research.** Relying upon domestic and the world practices, as well as scientific research [1-4], following basic factors, affecting the efficiency of underground coal gasification, can be singled out:

- mining and geological environment of the deposit occurrence;
- amount of water, involved into the gasification process;
- mineral composition of coal;
- characteristics of blast delivered to the gas generator; and
- arrangement of wells. The factors may be divided into controllable (those which can be varied during UCG process), i.e. blast characteristics, and arrangement of wells; and initial factors (which cannot be varied), i.e. mineral composition, and coal seam thickness.

Coal seam thickness, its depth as well as tectonic disturbance of enclosing rocks are among the mining and geological conditions affecting UCG process. Increased seam thickness results in the decreased heat loss in the environment, decreased specific water inflow, and ultimately, in the increased gas heat as well as gasification process efficiency.  However, specific gas output lowers due to the decreased seam mining as for its thickness. Thus, according to operation data of gas generators №№5, 5*a*,*b* and 6 of *Yuzhno-Abinskaia* station of *Podzemgaz* [5], gas heat output, obtained within *Vnutrenni IV* seam with 9 m thickness, is 1-1.5 MJ/m$^3$ higher to compare with *Vnutrenni VIII* seam with 2.2 m thickness. In this context, specific gas output is less by 1 m$^3$/kg and gasification efficiency of thicker seam is 10-15% higher.

Coal seam shallowness results in gas loss through overlying rocks; in turn, significant coal seam depth results in sharp efficiency decrease. Availability of faults, tectonic disturbances, and complicated seam hypsometry troubles the development of a reaction channel as well as control over a combustion source.  Less than 100 m depth of a coal seam occurring within undisturbed rocks is optimum for its mining by means of UCG technique making gasification process more stable [2].

In the process of UCG, water balance is formed of natural coal humidity, inflows of water to a gas generator, water, containing in the blast, and water, being formed in the process of carbon, hydrogen, and methane combustion as well as CO conversion. Low water within the coal as well as nonavailability of water inflows may results in moisture lack which will decelerate gasification process; among other things that gives rise to the decreased CO formation during reduction reactions. Much water decelerates coal seam degassing, and reduces heat content of gas, being generated, due to its increased water ratio (Fig. 1).

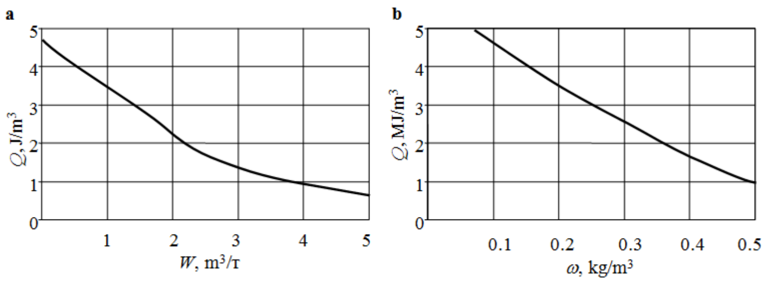


**Fig. 1.** Dependence of gas heat output ($Q$) upon: *a* - specific water inflow to the seam ($W$); and *b* - gas water content ($\omega$)

Hence, the amount of water, involved in UCG process, should be controlled strictly depending upon specific conditions. The main procedures to control amount of water, participating in UCG process, are: preliminary dewatering of a deposit by means of drain wells; increased pressure of the blast to displace moisture from the gas generator; increased oxygen content within the blast; and increased air to be supplied.

Changes in characteristics of blast, delivered to the gas generator as well as chemical content of the blast, delivery rate, and delivery pressure are the important factors effecting gasification procedure [6-7]. Analysis of the results of coal seams gasification shows that blast oxygenation increases temperature within combustion area; delocalizes it; and intensifies heat output of the gas, being generated. If oxygen content of the blast to be delivered is two times higher than atmospheric one, then the content of CO and $H_2$ experiences 1.5 to 2 times increase. Water vapour with 0.15-0.2 kg/m$^3$ content added to air blast (within the drained deposits) intensifies reduction reactions increasing CO, $H_2$, and $CH_4$ output. Combined use of oxygen and water vapour (i.e. vapour-oxygen blast) is more efficient. A Table demonstrates the influence of blast content on the heat output of the generated gases in the context of different UCG stations.

Experiments, concerning the effect of blast intensity on the gasification process were carried out within gas generator #1 of *Yuzhno-Abinskaia* station of *Podzemgaz* during its different operation periods. To begin with, blast consumption was increased from 1000 to 6500 m$^3$ per hour; then, it was decreased gradually from 6500 down to 1000 m$^3$ per hour. Fig. 2 explains changes in the content and gas heat output in terms of various consumption of blast delivered for gasification.

The graph demonstrates that gas heat output increases depending upon the increase in the blast consumption. Moreover, the increase in heat value depends on carbon monoxide mainly. Carbon dioxide content within the gas reduces moderately while blast intensity increasing; at the same time, content of other components remains constant being more or less independent of the blast consumption.

Experiments have determined [8] that in addition to the blast intensity, interrupted blast to a reaction channel is one of the factors intensifying heating value of gas as well as the efficiency of UCG station. Fig. 3 represents a graph of changes in gas composition in the context of Gorlovka *Podzemgaz* station.

Table 1

Influence of the blast chemical composition on the gas heat output

| Blast type | Station | Gas heat output, MJ/m$^3$ |
|---|---|---|
| Air blast | Lisichanskaia | 3.1 |
| | Podmoskovnaia | 3.6 |
| | Yuzhno-Abinskaia | 4.6 |
| Oxygen blast | Lisichanskaia | 5.3 |
| | Podmoskovnaia | 7.3 |
| Vapour-air blast | Yuzhno-Abinskaia | 6.3 |
| Vapour-oxygen blast | Podmoskovnaia | 6.8 |

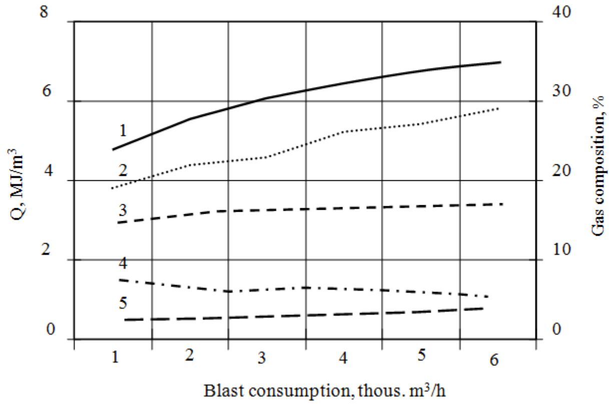

**Fig. 2.** Changes in gas heat output *Q* (1) and its composition CO (2), $H_2$ (3), $CO_2$ (4), $CH_4$ (5) in terms of various blast types

When gasification channel operated with the use of air blast (section *A*), $H_2$+$CH_4$ content within the gas was 15-18% in the context of 4.8 MJ/m$^3$ average heating value. After blast was interrupted to the gasification channel, intensive increase in $H_2$+$CH_4$ content started; the increase continued during the whole blastless period (section *B*). Then, when blast was restarted, composition of the gas, being generated, varied sharply. After 80 minutes it came up to the level when the channel operated with the use of air blast, i.e. $H_2$+$CH_4$≈15-18 % (section *C*). During blastless period, the peak $H_2$+$CH_4$ content was 58%, and heat output was up to 11 MJ/m$^3$.

Ash washing off coal surface, decreased aerodynamic drag factor, and increased coal loosening are the advantages of pulsating blast delivery. Use of the technique intensifies a process of gas release, and reduces the influence of negative factors arising with uniform blast.

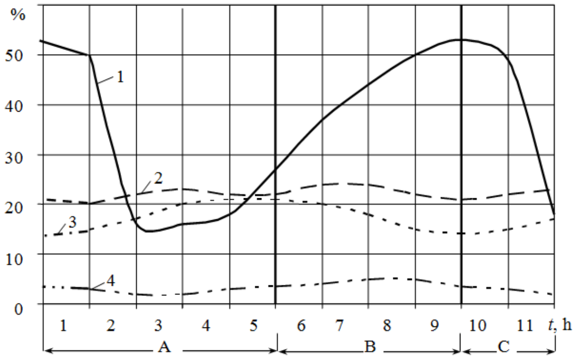


**Fig. 3.** Changes in the concentration of gas components (*1* - $H_2$; *2* - $CO_2$; *3* - CO; *4* - $CH_4$) during blast and blastless periods of underground gas generator operation

Effect of static pressure within gas generator on gas heat output and loss value was analyzed at *Podmoskovnaia* station of *Podzemgaz* during 1954-1956 [9]. During the period, static pressure varied significantly; averaged data can help estimate its change influence (Fig. 4). As it is seen in the graphs, increased pressure results in the increased heat output as well as in the increased gas loss. Average $10^4$ Pa pressure increase results in 0.25 $MJ/m^3$ gas heat output increase and in 5% gas loss increase.

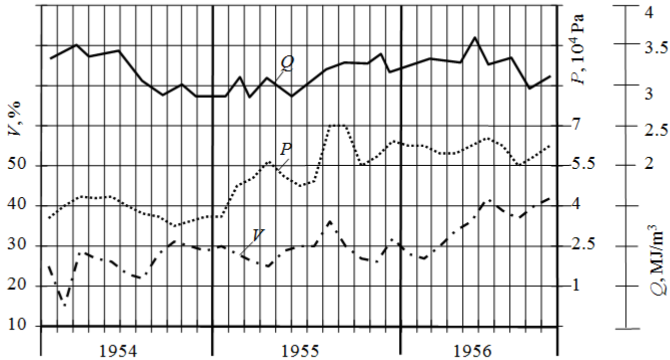


**Fig. 4.** Changes in static pressure (*P*), heat output (*Q*), and gas loss (*V*) in Podmoskovnaia station of Podzemgaz

Fig. 5 shows changes in gas humidity depending upon static pressure. Increase of static pressure results in certain forcing out of formation water owing to which moisture content of the gas reduces. The data confirm the dependence of the increased pressure upon the increased heat output. Moreover, high static pressure within gas generator prevents from rock roof caving and reaction channel filling up with molten rock.

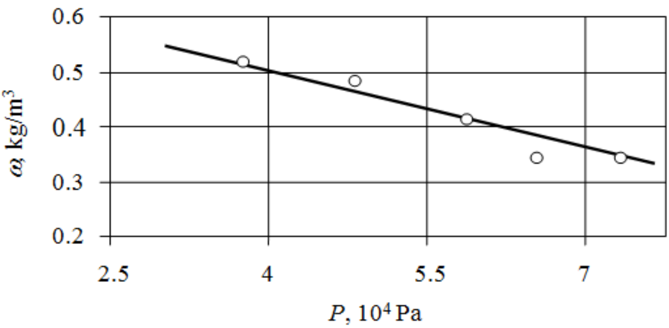


**Fig. 5.** Dependence of gas humidity ($\omega$) upon static pressure ($P$)

**Analytical approach to study temperature field distribution within rock mass during underground coal gasification (UCG).** It is known that modes of conductive and convective rock mass heating may arise within underground gas generator in terms of different underground water pressure-gas pressure ratios. Consider a situation when pressure within gas generator is less than water pressure; thus, gas effusion doesn't originate and heat transfer is of conductive nature, mass transfer with surrounding rock mass is minimal being carried out at the expense of diffusion.

In terms of static position of two rock mass phases (i.e. rock+water), thermal flow from gas generator may be reduced to axisymmetrical consideration of temperature field described by an equation of the type [11]

$$T(r,t)-T_0=\frac{q}{\lambda}R_2\left\{\frac{R_2^2}{R_2^2-R_1^2}\left[2\frac{at}{R_2^2}-\frac{1}{4}\left(1-2\frac{r^2}{R_2^2}\right)-\frac{R_1^2}{R_2^2}\left(\ln\frac{r}{R_1}+\frac{R_2^2}{R_2^2-R_1^2}\ln\frac{R_1}{R_2}+\frac{3}{4}\right)\right]+\right.$$

$$\left.+\sum_{n=1}^{\infty}\frac{\pi}{\mu_n}\frac{I_1\left(\mu_n\frac{R_1}{R_2}\right)I_1(\mu_n)}{I_1\left(\mu_n\frac{R_1}{R_2}\right)I_1(\mu_n)}\cdot\left[I_0\left(\mu_n\frac{r}{R_2}\right)Y_1\left(\mu_n\frac{R_1}{R_2}\right)-Y_0\left(\mu_n\frac{r}{R_2}\right)I_1\left(\mu_n\frac{R_1}{R_2}\right)\right]\cdot e^{-\mu_n^2\frac{at}{R_2^2}}\right\} \quad (1)$$

where $q$ is specific heat flow capacity; $R_1$ and $R_2$ are radius of a gas generator radius and its depth relative to earth's surface respectively; $r$ is distance from the gas generator axis to a reference point; $t$ is time baseline period; $T_0$ is background rock mass temperature; $\mu_n$ are characteristic first-order numbers of Bessel function for boundary values $R_1$ and $R_2$; $\lambda$ is heat conductivity factor of water-saturated rock mass.

Heat-transfer problem considering relative displacement of one of the rock mass phases in the context of analytical version is extremely difficult.

One-dimensional solution in terms of finite differences for static case and taking into consideration liquid phase transfer is represented by means of the equations

$$T_i^t=\frac{1}{2+\frac{\Delta x^2}{a\Delta t}}T_{i-1}^t+\frac{1}{2+\frac{\Delta x^2}{a\Delta t}}T_{i+1}^t+\frac{\Delta x^2}{2a\Delta t}T_i^{t-\partial t} \quad (2)$$

$$T_i^t=\frac{\frac{\lambda}{\Delta x^2}-\frac{C_wV_w}{\Delta x}}{\frac{C_r}{\Delta t}-\frac{C_wV_w}{\Delta x}+\frac{2\lambda}{\Delta x^2}}T_{i+1}^t+\frac{\frac{\lambda}{\Delta x^2}}{\frac{C_r}{\Delta t}-\frac{C_wV_w}{\Delta x}+\frac{2\lambda}{\Delta x^2}}T_{i-1}^t+\frac{\frac{C_r}{\Delta t}}{\frac{C_r}{\Delta t}-\frac{C_wV_w}{\Delta x}+\frac{2\lambda}{\Delta x^2}}T_i^{t-\Delta t} \quad (3)$$

where $a$ is temperature conductivity coefficient; $Cr$, and $Cw$ are heating capacities of rock and water respectively; and $Vw$ is actual velocity of water flow; the mentioned specifications have already been involved.

To use the solutions correctly, certain features of the set problem should be mentioned.

Nonlinear temperature within axisymmetrical thermal flow is: temperature gradients decay at the distance of 3-4 radii of a thermal source reduced to a cylindrical form. In the context of the layer, practical evaluations can not involve difference between one-dimensional and axisymmetrical flows.

Formula (1) is true for boundary second-type conditions when a function of a heat flow is known. In terms of sensible temperature difference between thermal source ($T_s$) and absorptive medium ($T_0$), the function becomes constant

$$q = \sigma \cdot C(T_s - T_0)\,, \tag{4}$$

where $\sigma$ is Stefan-Boltzmann constant; and $C$ is a coefficient depending upon capability of the medium to absorb thermal energy.

Underground gas generator emits thermal flow which temperature achieves 1000°C; as a rule, it means that condition (4) has been applied. It is obvious that within rock masses, being typical for coal deposits, a value of thermal flow according to condition (4) can be obtained from equation (1) on the experimental temperature measurements. To do that, use actual data from [12].

Results of variant calculations of dynamics of a temperature field in roof rocks of an underground gas-generator, confirmed by convergence with the actual data [12] create a possibility to evaluate the influence of hydrogeological conditions on it more differentially. The highest temperature distribution indexes in a five-meter contour are typical for a condition of rocks at natural humidity, i.e. when a massif is pre-drained. The smallest range of distribution of a temperature field is typical for conditions of water-saturated filtration flow at a filtration rate of 0.4 m/day, which is typical for location of sandstone rocks in a roof of a gas-generator. The study of distribution of a temperature field allows applying accurate corrections to change in physical and mechanical properties of rocks when creating numerical mathematical models.

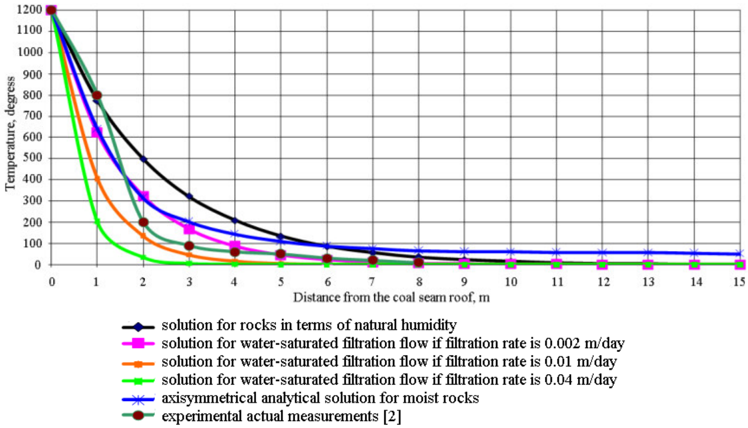


**Fig. 6.** Demonstrates results of variants calculations showing dynamics of temperature field within roof rocks of underground gas generator

## Experimental procedure and results of the experiments in the context of physical modeling

Experimental module to study a process of distribution of temperature field of overburden rocks and their permeability (Fig. 7) was developed and manufactured taking into consideration the calculated similarity coefficients. Modeling of coal seam degassing process was performed within clear thermal-resistant tube with 1 m length and 0.04 m diameter. Compressor was used to supply air into combustion chamber. Air consumption was similar during the whole experiment. Pressure difference was recorded with the help of a manometer; temperature was recorded with the help of microthermocouple elements. Temperature within a medium being modeled (i.e. fine sand) was controlled from a combustion zone to combustion products extracted to atmosphere through a hydroseal. Gas consumption was recorded with the help of flow rate meter.

Source excess pressure providing air supply while igniting, was $1.013 \cdot 10^5$ Pa. The ignition was provided by means of thermal heat of coal. After the coal started firing, the ignition device removed and combustion rate was supported with the help of air supply. After filtration, the gas was extracted through a hydroseal to the atmosphere [6].

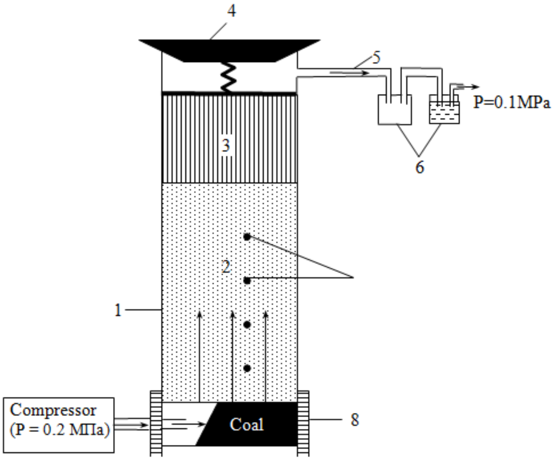


**Fig. 7.** Scheme of experimental facilities: *1* – clear thermal-resistant tube; *2* – roof rock of a coal seam (sand); *3* – laboratory cotton; *4* – a stopper; *5* – interconnector; *6* – moisture collector and hydroseal; *7* – thermocouple elements; and *8* – ignition device

The experiment involved visual observation of changes in the state of the coal seam and overburden rocks. Its period was limited by time of coal combustion (i.e. 45 minutes); then the medium, which has already been saturated by gasification products, is ejected from the thermal-resistant tube for the analysis of filtration properties.

To evaluate filtration parameters of the medium, its particle composition was studied with the help of grain-size analysis. Since effective diameter is 0.1 to 3 mm and heterogeneity coefficient is less than 5, nomogram of N.N. Bindeman has been applied to determine a filtration coefficient of the medium being modeled [13-14]. A value of the filtration coefficient was $\kappa_f$ =3 m/day. Permeability coefficient $k_p$ has been identified according to the dependence [15]

$$k_p = \frac{k_f \cdot \mu}{\rho \cdot g}, \qquad (5)$$

where $k_f$ is filtration coefficient; $\mu$, and $\rho$ are dynamic viscosity and water density. The calculated value of sand permeability within the experimental facilities was determined as $4.46 \cdot 10^{-11}$ m$^2$.

Permeability coefficient was also evaluated according to data obtained during the experiment relying upon formula (6) [16]

$$\kappa_p = \frac{2\mu P_{at} QL}{F\left(P_1^2 - P_2^2\right)}, \tag{6}$$

where $P_{at}$ is atmospheric pressure ($1.013 \cdot 10^5$ Pa); $Q$ is consumption of air being pumped to a combustion chamber ($4 \cdot 10^{-5}$ m$^3$/s; $L$, and $F$ are a seam thickness and sectional area of overburden rocks (0.5 m and $1.25 \cdot 10^{-3}$ m$^2$); $\mu$ is average dynamic viscosity of filtering gas ($1.481 \cdot 10^{-5}$ Pa·s); and $P_1$, and $P_2$ are intake pressure and output pressure on the exit from a layer of gas-permeable rocks respectively ($2.026 \cdot 10^5$ Pa and $1.013 \cdot 10^5$ Pa).

The $k_p$ value, determined on (6), was $3 \cdot 10^{-12}$ m$^2$. Difference between the obtained values of permeability coefficient is allowable taking into consideration empiric data of granular sand composition. The obtained experimental value should be used in the context of subsequent calculations.

In the course of the experiment, temperature was recorded in certain points of the model at the distances of 5, 10, 12, 15, and 20 cm from the combustion source. The temperature was recorded continuously with the help of identical thermal couples connected to multichannel recorder H-307. The thermal couples have been calibrated relative to hyperthermal temperature gauge ТУ-31А № 433 with ±2 °C error. Figures 8 and 9 demonstrate over-time temperature variations within the filtering medium.

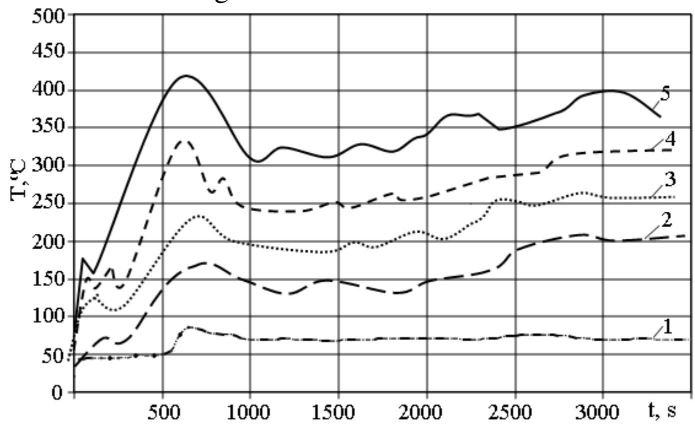


**Fig. 8.** Temperature variations within the filtering medium: 1,2,3,4 and 5 are temperature variations in a roof at the distance of 20, 15, 12, 10, and 5 cm from the top edge of the combustion zone respectively

The coal seam state as well as overburden rocks state was observed visually synchronous with temperature recordation; as a result, the following was determined:

- a zone of coal combustion is convex towards air motion; its geometry depends upon a supply rate;
- combustion zone-overburden rocks contact is unstable; overlying sand material penetrates into the combustion zone;
- in due course, the filtering medium (i.e. sand material) becomes grey with point distribution of black microinclusions;
- through the microscope, films of resinous substances, thickening within irregularities, are seen at the surface of the sand grains; and
- an arch is formed right above the zone of coal combustion; its stability depends upon the number of carboniferous inclusions and dimensions of the zone is determined with the help of the coal-combustion process duration.

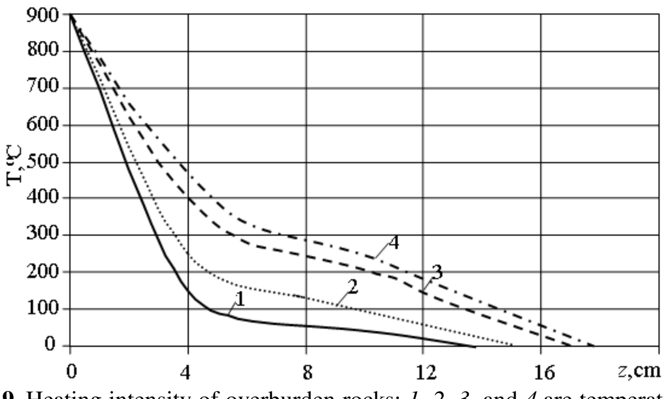


**Fig. 9.** Heating intensity of overburden rocks: *1*, *2*, *3*, and *4* are temperature distribution within a roof after 200, 400, 600, and 2500 s from the experiment beginning respectively

The data, obtained during the experiments, have helped conclude that rocks of immediate roof, occurring closer to the combustion zone, become of higher temperature and start varying first. Temperature increase within overburden rocks is followed by changes in their physical and mechanical characteristics. After rock heating, evaporation of natural and bound moisture starts. The evaporation originates at the temperature of 100 °C; when the temperature achieves 200 $^0$C and exceeds it, chemical moisture is liberated from roof rocks. Temperature increase up to 600 °C results in agglomeration and further decomposition of certain elements of overburden rocks (Fig. 10).

**Fig. 10**. Samples of sandy deposits and argillaceous deposits of Dnieperbas after 400 °C and 650 °C temperature field effect on rock mass

Analysis of curves (Fig. 7 and 8) means that roof rock heating process is intensive during the first 600 seconds from coal ignition within a combustion zone. Further heat transfer is a very slow process. The phenomenon can be explained by the fact of the decreased thermal conductivity of overburden rocks at the expense of changes taking place in their physical state (i.e. agglomeration, expansion, pore mudding) under the effect of high temperature and chemical effect of escaping gas. Insignificant temperature variations during the experiment can be explained by the unstable burning process and, consequently, temperature fluctuations within inlet boundary.

In the context of the medium, being modeled, vertical temperature distribution is nonlinear process. Distribution of temperature within certain areas (Fig. 8) corresponds to the processes of rock variations, condensation of filtering gas, and circulation of gas flows with constant temperature.

Both physical and filtration properties of the medium, saturated during the experiment, were calculated and determined from its different areas by means of a technique of cutting cylinders [10]; Table 2 contains the results.

The analysis shows that migration of gasification products (GP) within filtering medium results in nonuniform filling of pore space with the formation of several zones. First of all, GP distribution depends upon temperature distribution. Poriness of overburden rocks and their permeability vary owing to mechanical blocking of pores by means of unburnt combustibles as well as physical and chemical *GP-rock* interaction. A zone of thermally altered rocks with solid carboniferous inclusions is the closest to the degassed area. In consideration of geometrical similarity coefficient ($C_1$=25), thickness of the zone will not be more than 0.5 m under full-scale conditions. Above the zone (at the distance of 0.5-2.5 m) a condensation zone is located which porous space is filled with resinous products. Within the overlying zone of undisturbed rocks, constant-temperature gas flows circulate.

The determined regularities coincide qualitatively with the data obtained at Shahtinsk station *Podzemgaz* [18, 19]. Thus, after gasification of a coal seam *Rozovy* with 0.4 m thickness, upper share of overburden rocks was melted layer containing unburnt combustibles with up to 20 cm thickness. Above the layer (at the distance of 0.2-1.5 m) rocks transferred gradually from melted (i.e. red colour) to undisturbed (deep blue ones).

Table 2

Structure and properties of overburden rocks saturated by gasification products (according to the data of physical modeling)

| Zone | Distance from a coal seam roof, m | Prevailing processes | Permeability, $m^2$ | Poriness, % | Density, $kg/m^3$ |
|---|---|---|---|---|---|
| 3 | >2.5 | Filtration gas flow (undisturbed rocks) | $3 \cdot 10^{-12}$ | 33 | 1510 |
| 2 | 0.5-2.5 | Filtering gas condensation (pores are filled with liquid carbohydrates) | $1.6 \cdot 10^{-12}$ | 27 | 1630 |
| 1 | <0.5 | Rock melting (slagged and agglomerated rock with the inclusion of unburnt combustibles) | $9.2 \cdot 10^{-13}$ | 21 | 1740 |

Temperature above the layer being characterized was 700-800 °C; it dropped gradually down to 500 °C. Then, the temperature became

150-200 °C within a zone where the rocks transferred from heat-dried state to water-saturated one.

Zones of immediate roof annealing of *Rozovy* coal seam were located closer to a rock boundary of the underground gas generator to compare with the zones selected for the experiment. Their eliminating can be explained by slower decrease in the parameters of gas being filtered within the medium under modeling (sand material) and, consequently, by its greater permeability and heat transfer to compare with *Rozovy* seam roof (shale).

**Numerical modeling of filtration parameters in the context of two-layer rock formation within a roof of a gas generator**

If a coal seam roof contains water-proof argillaceous rocks (even with carbonaceous component) and up to 0.01 m/day values of filtration coefficient being typical for them (Fig. 11), the values of specific water inflow in the context of shear deformations of the rock formation [10,20] are within 0.11-0.23 $m^2$/day when gas generator operates.

The evaluation of changes in hydrodynamic mode of the complicated rock formation, containing gas generator, has shown that formation of filtration parameters depends directly on the changes in rock lithology under the effect of temperature field, geomechanical processes, and residual hydraulic pressure.

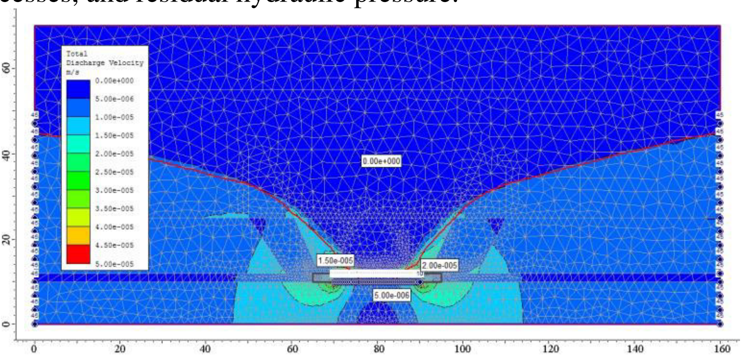


**Fig. 11.** Distribution of filtration rates within foliated rock mass disturbed by operation of the gas generator if waterproof layer is available within a roof of a coal seam, m/s

On the basis of numerical simulation, under conditions of a complex lithological structure of roof rocks [21], it is possible to determine the values of specific water inflows into the channel of a gas-generator at various stages of its formation with sufficient accuracy. The solution of this problem is possible only with a complex approach based on previously obtained data on the transformation of physical and mechanical properties of rocks under the influence of temperatures, and a change of geofiltration parameters in a geomechanically disturbed massif.

**Conclusions**

1. The studies concerning the factors, working upon the efficiency of underground coal gasification, have shown that perturbing factors are not equal to controlling ones in terms of their degree of influence. All the perturbing factors with the exception of a coal seam thickness have an adverse effect on gas heating power; in turn, blast characteristics are the most favourable ones among controlling factors. Hence, increased blast consumption and increased static pressure within a gas generator are the most active controllable factors working on the efficiency of UCG process. Conversely, that results in the increased gas loss which may decrease both profitability and environmental safety of UCG.

2. It is established that the zone of intensive thermal transformation of rocks reaches 2.5 m, which is confirmed by the results of physical simulation. The decrease of the temperature field to 100°C occurs in an interval from 1.5 to 4.5 m, and is non-linearly distributed vertically. These patterns coincide qualitatively with the data obtained at Shakhtynska station of "Podzemgaz".

3. The temperature increase in covering rocks is accompanied by a change in their physical and mechanical characteristics. Evaporation of natural and bound water begins after the warming of rocks. At a temperature above 200 °C, the release of chemical moisture from the roof rocks begins, and a temperature increase to 600 °C leads to sintering and further disintegration of individual components of covering rocks and a change in their permeability.

4. The physical modeling results have helped determine permeability coefficient for different roof zones above gasification channel. Difference between the obtained values of the permeability coefficient is allowable on the basis of granular sand composition.

5. Zones with different permeability have been determined and values of specific water inflow have been identified basing upon the performed numerical modeling and involving multicomponent transformations within roof formation.

*References*


1. **Korolev, I.V.** (1962). Dependence of the UCG process on geological and hydrogeological conditions at coal deposits. VNIIPodzemgaz, nauchnyye trudy. Podzemnaya gazifikatsiya ugley. № 8, 64 – 70.

2. **Yefremochkin, N.V**. (1960). Features of the groundwater regime in terms of coal gasification at the Shatskoye field. VNIIPodzemgaz, nauchnyye trudy. Podzemnaya gazifikatsiya ugley. № 3, 29 – 33.

3. **Yudin, I.D., Grigor'yev, V.V.** (1958). Underground gasification of coal in Kuzbass. Moskva. Ugletekhizdat, 28.

4. **Saik, P., Petlovanyi, M., Lozynskyi, V., Sai, K. and Merzlikin, A.** (2018). Innovative Approach to the Integrated Use of Energy Resources of Underground Coal Gasification. Solid State Phenomena, 277, 221-231.

5. **Nusinov, G.O., Brushteyn, N.Z., Kulakova, M.A., Dotsenko, P.N.** (1963). Underground gasification on the water-filled areas of a coal seam. VNIIPodzemgaz, nauchnyye trudy. Podzemnaya gazifikatsiya ugley. № 9, 85 – 88.

6. **Arinenkov, D.M., Markman, L.M.** (1960). Underground coal gasification. Donbass: Knizhnoye izdatel'stvo Stalino. 94.

7. **Inkin, O., Dereviahina, N**. (2018). Study of the migration processes in the roof of an underground gas-generator. Dniprop. Univer. bulletin, Geology, geography. 26 (1), 64-70.

8. **Kulish, Ye. D.**, 1958. Underground gasification of Moscow brown coal. Moskva. Ugletekhizdat. 36.

9. **Garkusha I. S**. 1964. Podzemnaya gazifikatsiya uglya [Underground coal gasification]. Trudy instituta i proizvodstvennyy opyt. Moskva. Nedra. №12, 36. (in Russian).

10. **Sotskov, V.O., Demchenko, Yu., Salli, S.V. & Dereviahina N.I.** (2017). Optimization of parameters of overworked mining gallery support while carrying out long-wall face workings. Naukovyi Visnyk Natsionalnoho Hirnychoho Universytetu. №6, 34-40.

11. **Russo, Yu.V.** (1957). Heat losses in the side rocks during the underground gasification of thin gentle and inclined coal seams. Podzemnaya gazifikatsiya ugley, (5).

12. **Kreynin, Ye.V.** (2004). Non-traditional thermal technologies for the extraction of hard-to-recover fuels: coal, hydrocarbons. Moskva: OOO "IRTS Gazprom".

13. **Tishkov, V.V.** (2014). Assessment of water inflow into the channel of an underground gas generator, when changing the permeability parameters of the massif, in the conditions of the Dnieper basin. Mining of Mineral Deposits. 8(4), 409-413. https://doi.org/10.15407/mining08.04.409

14. **Sadovenko, Í.O., Timoshchuk, V.Í., & Tíshkov, V.V.** (2010). Investigation of the influence of the stress-strain state of the host rocks on their filtration properties during underground gasification of coal seams. Naukovyi Visnyk Natsionalnoho Hirnychoho Universytetu, (3), 32-33.

15. **Sadovenko, I.A., Polyashov, A.S., & Inkin, A.V**. (2004). Experimental studies of the mechanism of filtration of gasification products. Gírnichodobuvna

promislovíst Ukraïny í Polshchí: Aktualní problemy í perspektivy: Mater. Ukraïnsko-Polskoho forumu hírnykív, 598-603.

16. **Mironenko, V.A.** (1983). Groundwater Dynamics. Moskva: Nedra.

17. **Semenenko, D.K., Russa, Yu.V., & Ovchinikov, V.M.** (1959). Gas permeability of a gas-filled space filled with slagged rocks. Podzemnaya gazifikatsiya ugley, (4), 19-21.

18. **Lomtadze, V.D.** (1952). Laboratory methods for the physicomechanical properties of sandy and clay soils. Moskva: Gosgeolizdat.

19. **Skafa, P.V.** (1960). Underground Coal Gasification. Moskva: Gosgeolizdat.

20. **Sotskov, V.O., Demchenko, Yu. I., Salli, S.V., & Dereviahina, N.I.** (2017). Optimization of parameters of overwoked mining gallery support while carrying out long-wall face workings. Naukovyi Visnyk Natsionalnoho Hirnychoho Universytetu, (6), 34-40.

21. **Fomichov, V., Sotskov, V., Pochepov, V., & Mamaikin, O.** (2018). Formation of a calculation model determining optimal rate of stoping face movement with a large deformation of a rock massif. ARPN Journal of Engineering and Applied Sciences, 13(7), 23 81-2389.

22. **Sotskov, V., & Saleev, I**. (2013). Investigation of the rock massif stress strain state in conditions of the drainage drift overworking. Annual Scientific-Technical Collection - Mining of Mineral Deposits, 197-202. https://doi.org/10.1201/b16354-36.